Improved Network Coverage with Adaptive Navigation of mmWave-based Drone-Cells

Nikita Tafintsev†, Mikhail Gerasimenko†, Dmitri Moltchanov†, Mustafa Akdeniz⋆,
Shu-ping Yeh⋆, Nageen Himayat⋆, Sergey Andreev†, Yevgeni Koucheryavy†, and Mikko Valkama†
†Tampere University of Technology, Tampere, Finland
⋆Intel Corporation, Santa Clara, CA, USA.

***Abstract*—The use of drone-cells in 5G wireless systems is a topic of ongoing discussions in the 3GPP standardization community. A major advantage of employing drones is that they can dynamically and timely improve the capacity and coverage of cellular networks. To address this challenge, efficient network planning tools targeting spontaneous and rapidly changing scenarios for dynamic network design need to be developed. Complementing the recent studies on the optimal static drone-cell positioning for a Poisson point process of user equipment (UE) placement, we study UE distributions with correlated mobility models. We first derive the coverage metrics for static drone-cell deployments and then proceed by developing an algorithm for adaptive drone-cell navigation. Considering the mean number of covered UEs, we show that enabling drone-cell navigation improves the overall system performance.**

I. Introduction

The recent progress in design of light-weight drones, or unmanned aerial vehicles, has made them suitable for utilization in a wide range of civilian fields including surveillance, delivery services, and agriculture, among others. One of the emerging applications of drones currently being studied within the 3GPP community is their use as a platform for small cells in wireless networks [1], [2].

The key benefit of drone-based small cells is to timely and dynamically provide or improve the network capacity by moving them to the location with the temporarily increased traffic demands. There are two options for using drone-based cells in a particular scenario. Under no information about the user equipment (UE) locations, one can apply conventional terrestrial radio network planning (RNP) tools to deploy drones as a hexagonal grid according to the appropriate coverage and capacity demands. In this case, drones hover for a longer time over specific areas without the need for navigation. In the second case, drones assume to know the geographical position of each UE and continuously adjust their locations by following the UE traffic demands [2], [3].

A. Related Work

The recent studies of drone-cell deployment strategies primarily target their optimal positioning to service stationary UEs. Particularly, the authors in [4] followed an analytical approach to obtain the optimal altitude of a Low Attitude Platform (LAP) maximizing the coverage metrics. In [5], the authors solved a 3D positioning problem for drone-cells. The authors in [6] considered the use of drones to provide emergency coverage over a disaster area in the presence of LAPs. The drone-cell coverage problem solved in [3] has been formulated to maximize the coverage range under the minimum transmit power. The authors also investigated the impact of interference in a scenario with two drone-cells.

In [7], the authors addressed 3D optimal positioning of drone-cells to cover a number of UEs by using a heuristic approach based on a particle swarm optimization (PSO) algorithm. They established that in a dense area, it is beneficial to decrease drone altitudes thus limiting the interference for the farther away UEs, which are served by another drone-cell. In low-density regions, it is preferable to increase the altitude thus covering a larger area and serving more UEs. The authors in [8] addressed the deployment of multiple drone-cells with directional antennas. They derived the downlink coverage of a drone-cell as a function of the altitude and the antenna gain as well as determined the locations of the drone-cells, such that the total coverage area is maximized.

The authors in [9] investigated the optimal 3D positioning of drone-cells over an urban area by taking into account their backhaul requirements. Finally, the aspect of dynamic re-positioning has been addressed in [10], where the authors proposed a distributed algorithm for dynamic adaptation of drone-cell positions and analyzed the associated spectral efficiency performance. Particularly, they showed that adaptive navigation may increase the spectral efficiency by almost 100% for realistic drone speeds and flight altitudes. In [11], the authors compared adaptive navigation with a static deployment of drone-cells by using a set of performance metrics of interest. They also proposed three simple algorithms for autonomous navigation.

Despite significant efforts devoted so far to address the optimal drone-cell positioning strategies, the reported studies have a number of common limitations. First, in most of past work, static UE deployment strategies have been assumed. This naturally leads to static solutions for drone-cell positioning as well. Further, the impact of optimal positioning on spectral efficiency has to be analyzed before any decisive conclusions can be made.

B. Our Contribution

This paper aims to develop an adaptive drone-cell navigation scheme and compare its performance against static drone-cell

deployments under various UE mobility patterns. Our metric of interest is the mean number of covered UEs.

The main contributions of this work are as follows:

- we evaluate the coverage performance of drone-cells for a random direction mobility (RDM) model of UEs and develop, as a comparison, an analytical model assuming static deployment of drone-cells, by addressing different drone-cell deployment strategies;
- we investigate the impact of adaptive navigation of drone-cells and design an optimization algorithm, which navigates drones by taking into account the UE relocations and appropriate changes of the received signal quality;
- we compare static and dynamic drone-cell deployment strategies for different types of mobility models and demonstrate that adaptive navigation is beneficial when UEs tend to cluster in groups.

The rest of this paper is organized as follows. In Section II, we introduce our system model. We assess the performance of static drone-cell deployments under various mobility patterns as well as introduce an adaptive drone-cell navigation algorithm in Section III. Numerical results are reported in Section IV. Conclusions are drawn in the last section.

II. System Model

In this section, we outline our system model. First, we introduce the considered scenario and then proceed by specifying the sub-models including the mobility of UEs, antenna and channel parameters, as well as drone-cell deployment strategies.

A. Considered Scenario

In this paper, we are interested in the scenarios where the spatial density of UEs varies over time. An example of such a use case may be a large-scale crowded event, for example, a festival or a concert. During this type of an event, people are distributed evenly over a particular area, or stand beside the stage during a concert.

Here, we consider the case where the event is starting/ending, and people are moving to the appropriate area. In this situation, people accumulate near the stage/exit, and a queue is created. At the same time, people are initially distributed uniformly across the scenario, and their correlated movement might create congestion or a higher density of UEs in a certain location. In such scenarios, most people assemble in groups and follow one direction, despite the variations in their individual trajectories (Fig. 1).

In what follows, M and N denote the numbers of drone-cells and UEs, respectively. The drone-cell altitude h_D is assumed to be constant, thus resulting in a well-defined coverage of radius R. The area to be covered is denoted by S_A, while N drone-cells cover the area of exactly S_C. For the group mobility model, we assume that each cluster comprises $N_{U,1}$ UEs, where 1 stands for one cluster, while the number of clusters is N_C. We are interested in the mean value of a random variable V_C denoting the number of UEs covered by drone-cells.

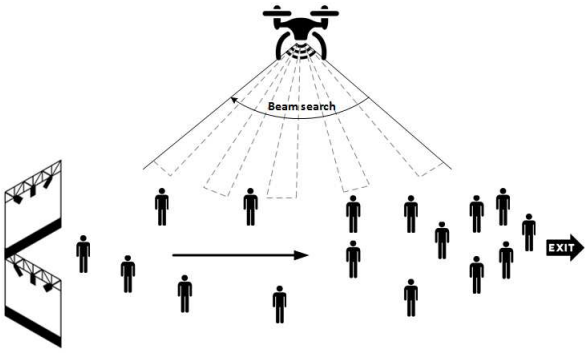

Fig. 1: Our considered "concert" scenario.

B. Mobility Models

By concentrating on the UE dynamics, we consider two inherently different mobility patterns: RDM model [12] and Reference Point Group Mobility (RPGM) model [13]. The former is used to address the case of random UE dynamics that captures the essentials of random movement and still preserves analytical tractability. According to RDM, a UE first randomly chooses the movement direction uniformly in $(0, 2\pi)$ and then travels in this direction at a constant speed of v_B for an exponentially distributed time with the parameter $\nu_B = 1/E[\tau_B]$, where τ_B is the mean duration of the movement. Here, the movements of UEs are independent, i.e., the speed and direction of one UE are not affected by other UEs.

In realistic scenarios, a single UE trajectory is often correlated with the others. For example, in a fair or a festival, UEs are concentrated around different attractor points and move between them in groups, which results in non-uniform density across the considered distribution. Hence, their mobility may be influenced by other UEs and by certain distribution parameters. The model we consider for this case is RPGM. Accordingly, each group of UEs has either an independent cluster center or a group leader. The movement of the group leader/cluster center defines the mobility behavior (direction) of the entire group. In our scenario, we assume that each group has a cluster center.

In RPGM model, the movement of a cluster center at time t can be denoted by a movement vector $\vec{V}^t_{group}$. Each member of the group deviates from this general movement vector $\vec{V}^t_{group}$ by some degree. Mobility of each member is defined by a reference point that follows the group movement. Formally, the motion vector $\vec{V}^t_i$ of a group member i can be described as

$$\vec{V}^t_i = \vec{V}^t_{group} + \vec{M}^t_i, \tag{1}$$

where $\vec{V}^t_{group}$ is the vector of the cluster center movement and $\vec{M}^t_i$ is the random deviation vector for the group member i.

Group trajectories follow the RDM, while vector $\vec{M}^t_i$ comes from independent and identically distributed (i.i.d.) random variables. Its length is distributed uniformly within a certain

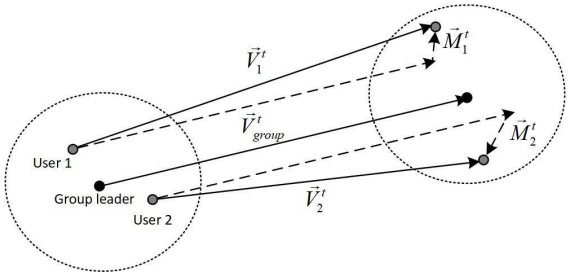

Fig. 2: Illustration of the RPGM model.

radius $[0, r_{max}]$ centered at the reference point, where r_{max} is the maximum allowed distance deviation, whose direction is distributed uniformly over the interval $[0, 2\pi]$. Fig. 2 illustrates a sample movement for the RPGM.

C. Antenna Array

In this work, we address millimeter-wave (mmWave) communications with directional antennas at drone-cells. At these frequencies, the radiation pattern of single-element antennas is relatively wide, while multi-element configurations often provide very narrow beamwidths [14]. In case of drone-cell applications, where the communication link may be oriented almost perpendicular to the ground surface, it is necessary to design antenna systems with high gain that have flexible directivity patterns to meet the appropriate communication demands for a mobile base station (BS).

To satisfy these requirements, we consider a planar array directed towards the ground, see Fig. 1, where the individual radiators are placed along a rectangular grid to provide equal coverage in all directions. Assuming an appropriate codebook configuration, the planar array's main lobe is steered towards any direction within the directivity pattern of an individual element. To model the array functionality for our scenario, we utilize the Fourier transform synthesis method described in [14].

For the sweeping procedure, which is required to steer both the TX and the RX arrays to positions, we use a simple signal strength-based full search algorithm. In the beginning, the UE is switching its antenna into an omnidirectional mode, where the array functionality is disabled. Then BS sends beacon messages in all possible array positions, and each UE saves the configuration index in which the received signal level was the highest. The procedure is repeated in the opposite direction (BS is switching to the omnidirectional mode, and UE is transmitting acknowledgments across all possible antenna configurations).

D. Channel Model

Most of the recent studies related to drone-cells consider an air-to-ground path loss model for low altitude platforms. According to [15], the ground station receives three groups of signals, including Line-of-Sight (LoS), strong reflected signals in terms of Non-Line-of-Sight (NLoS), and multiple reflected components, which cause multi-path fading.

In this paper, we consider the 3D mmWave stochastic channel model [16] suitable for drone-cells. It is based on ray-tracing data for urban-micro areas, where the path loss values were carefully adjusted by using the ray-tracing results and real-world radio measurements. The path loss is calculated as

$$PL = 20\log_{10}\left(\frac{4\pi}{\lambda_0}\right) + 10n_{pl}\log_{10}(d) + \sigma_{sf}, \qquad (2)$$

where λ_0 is the wavelength, n_{pl} is the path loss exponent, d is the distance in m, and σ_{sf} is the shadow fading. In this work, we consider only the LoS cases, by assuming that in our scenarios (a festival or a concert) the NLoS conditions are very rare. To take into account the multi-path signal components, we combine the aforementioned path loss with the multi-path channel model taken from [16].

E. Drone-Cell Deployments

Below, we consider three representative drone-cell deployment strategies: grid deployment, random deployment, and adaptive navigation.

In case of a grid deployment, drone-cells are hovering at certain locations that satisfy the coverage requirements. Coverage is defined here as a certain minimum signal-to-noise ratio (SNR) at the cell edge. The positions of drone-cells in a grid deployment are chosen to maximize the coverage area with minimum SNR, by assuming that coverage areas of drone-cells do not overlap. In case of a random deployment, drone-cells are assumed to be distributed uniformly over the area of interest. In the latter case, drone-cells are no longer static and may alter their positions during the service process according to a specified algorithm.

III. System Analysis

In what follows, we first address the case of static drone-cell deployments and then enable drone-cell mobility, since it may potentially lead to better system performance. We address both fixed grid and random drone-cell deployment strategies. The performance level for a static drone-cell deployment will then serve as a benchmark for adaptive optimization algorithms. We finally proceed with the description of our proposed time-dependent optimization algorithm.

A. Static Drone-Cell Deployment

1) RDM Model: First, consider independent mobility of all UEs according to RDM. In case of a fixed deployment, the coverage area of drone-cells, S_C, can be estimated by using zone of interest geometry and deployment positions. Note that we are interested in specific values of M and S_A, where $S_C < S_A$. The optimal fixed positions of drone-cells that provide full coverage can be established by using the well-known solutions for two-dimensional circle covering problem: see [17] for squares and [18] for circular areas.

Let M be such that $S_C < S_A$. Recall that the stationary distribution of RDM is uniform over the area of interest, $f(x, y) = 1/S_A$ [12], where x and y are the coordinates of the

UEs. When UEs move independently, the probability that exactly k UEs are covered in the steady-state, $q_k = Pr\{S_C = k\}$, is given by

$$q_k = \binom{N}{k} (1 - S_C/S_A)^k (S_C/S_A)^{N-k}, \; k = 0, 1, \ldots, \quad (3)$$

and the mean $E[S_C] = N(1 - S_C/S_A)$.

Consider now the static random deployment of drone-cells. The key difference as compared to the case of a fixed deployment is that S_C is now a random variable, while the coverage is stochastic. Let $f_{S_C}(x)$ be the probability density function (pdf) of the coverage area of S_A by M drone-cells. In this case, the probability that exactly k UEs are covered is

$$q_k = \int_0^{S_A} f_{S_C}(x) \binom{N}{k} \left(\frac{x}{S_A}\right)^k \left(1 - \frac{x}{S_A}\right)^{N-k} dx, \quad (4)$$

and the task reduces to finding the pdf $f_{S_C}(x)$.

Observe that the pdf $f_{S_C}(x)$ can be interpreted as the probability that a point uniformly distributed in the area of interest is covered. Consider first the case of $N = 1$. Denote by P a point of interest, by A_1 the coverage of a single drone-cell, and by A the area of interest. The sought probability, p_1, is then

$$p_1 = \frac{Pr\{P \in A \cap A_1\}}{Pr\{A \cap A_1 \neq 0\}}. \quad (5)$$

Using the notion of kinematic measure, we have

$$\begin{aligned} Pr\{P \in A \cap A_1\} &= m(A : P \in A \cap A_1), \\ Pr\{A_1 \cap A \neq 0\} &= m(A_1 : A_1 \cap A \neq 0), \end{aligned} \quad (6)$$

where the first expression is the kinematic measure for the set of motions of A, such that $P \in A$, while the second one provides the measure for all the motions of A, such that A_1 intersects A. For details, refer to [19].

The first measure is immediately computed to be

$$\begin{aligned} m(P \in A \cap A_1) &= \int_{P \in A_1} dx \wedge dy \wedge d\phi = \\ &= \int_{P \in A_1} dx \wedge dy \int_0^{2\pi} d\phi = 2\pi S_{A_1}, \end{aligned} \quad (7)$$

where S_{A_1} is the area of A_1.

The measure of all the motions of A, such that $A_1 \cap A \neq 0$, is [19]

$$\begin{aligned} m(A_1 \cap A \neq 0) &= \int_{A_1 \subset A} dx \wedge dy \wedge d\phi = \\ &= 2\pi[S_A + S_{A_1}] + L_A L_{A_1}, \end{aligned} \quad (8)$$

where L_A is the perimeter of A.

Substituting (8) and (7) into (5), the probability q_1 follows. Assuming that the drone-cells are deployed independently, the probability that a point is covered by at least one drone-cell out of M deployed ones is given by $p_M = 1 - (1 - p_1)^M$. Assuming that the zone of interest is a square with side B, we have

$$p_M = 1 - \left(1 - \frac{\pi R^2}{B^2 + \pi R^2 + 4BR}\right)^M, \quad (9)$$

which is interpreted as the fraction of area covered by M drone-cells.

The results in (3) and (4) hold for the stationary behavior. For time-dependent coverage, we have the following proposition.

Proposition 1 (Coverage)**.** *Assume that N UEs move in an arbitrarily shaped area according to RDM. Considering uniform independent initial distribution of the UEs at $t = 0$, the probability that at any t, $t > 0$, exactly k UEs are covered by M drone-cells with circularly shaped areas is given by (3) and (4) for fixed and random deployment of drone-cells, respectively.*

Proof. Observe that N uniformly distributed nodes in the area of interest can be interpreted as a conditional Poisson point process named Binomial process [20]. Since random displacements of an isotropic Poisson process are again Poisson [21], the result of the proposition immediately follows. □

An important corollary from the above is that there is no optimal movement trajectory for the deployed drone-cells that results in a better stochastic coverage of UEs.

2) RPGM Model: Consider again a fixed deployment of drone-cells. Observe that with respect to the mobility model, the centers of clusters move independently according to the RDM model, which leads to their uniform stationary distribution within the area of interest. Let $p_1^\star$ be a fraction of the cluster area inside the coverage area of the drone-cells. Observe that this fraction is obtained similarly to (5), which leads to

$$p_1^\star = \frac{Pr\{P \in B \cap B_1\}}{Pr\{B \cap B_1 \neq 0\}} = \frac{2\pi S_{B_1}}{2\pi[S_B + S_{B_1}] + L_B L_{B_1}}, \quad (10)$$

where B_1 is the coverage of drone-cells and B is the cluster.

Recall that each cluster is associated with $N_{U,1}$ UEs and the distribution in the cluster is assumed to be uniform. Given a certain coverage fraction of a cluster covered by drone-cells, the number of UEs falling into this fraction follows a Binomial distribution

$$\nu_k = \binom{N_{U,1}}{k} p_1^\star (1 - p_1^\star)^{N-k}, \; k = 0, 1, \ldots, \quad (11)$$

with the mean of $N_{U,1} p_1^\star$.

Since the clusters are assumed to move independently from each other, the fraction of UEs covered by statically deployed drone-cells at the fixed positions is given by $E[V_C] = N_{U,1} p_1^\star N_C$, where N_C is the number of clusters. Analyzing a random deployment, we observe that the only modification needed is to obtain the fraction of the area of the zone of interest covered by a random deployment of drone-cells. This has already been done in (9). The rest of the procedure is similar to that for the fixed deployment of drone-cells. We also note that the analysis above is precise when the overall area covered by the drone-cells constitutes a single convex set.

The results of this subsection deliver the steady-state coverage probabilities in a static random and fixed deployment of drone-cells. However, even if the exact positions of the UEs are known, with a large number of UEs under the i.i.d. mobility

assumption, it is not required to navigate the drone-cells to track any of these UEs, since the total number of covered UEs will not change during navigation to another point. However, with a small number of UEs or under a correlated mobility, the navigation of drone-cells will make a difference.

B. Adaptive Drone-Cell Navigation

To optimize the coverage for the case of the RPGM cluster-based model, we consider a PSO-based dynamic optimization approach. PSO is a heuristic computational algorithm that tackles the problem of dynamic optimization by iteratively attempting to improve a solution in relation to a given measure of quality. A candidate solution is a member of the set of possible solutions in the feasible region of a given problem. The algorithm solves a problem by having a population of candidate solutions and moving these particles around the search space. Each particle's movement is influenced by its local best-known position but is also guided toward the best-known positions in the search-space, which are updated as better positions are found by other particles. The algorithm is expected to move the swarm toward the best solutions.

The ultimate goal of our implementation of the PSO algorithm is to achieve maximum coverage. Assuming N UEs, the coverage constraint is formulated as

$$P(\gamma_{ij*} > \gamma) \geq \eta, \quad i = 1, ..., N, \tag{12}$$

where $j* = \text{argmax}\gamma_{ij}$, γ_{ij} is the SNR of the UE i receiving service from the drone-cell j, γ is the minimum SNR level required for each UE, and η is the proportion of all UEs covered by a drone-cell. The goal is to cover at least η percent of all the UEs.

The utility function is then

$$U = \begin{cases} \sum_{i=1}^{N} I_i & \text{if constraint holds,} \\ 0 & \text{otherwise,} \end{cases} \tag{13}$$

where

$$I_i = \begin{cases} 1 & \text{if UE is covered by drone-cell,} \\ 0 & \text{otherwise.} \end{cases} \tag{14}$$

The proposed algorithm is demonstrated in Algorithm 1.

Algorithm 1 PSO algorithm for the deployment of drone-cells

Generate a population consisting of L random particles $W^{(l)}(0), l = 1, \ldots, L$.
Each particle has the size of $3 \times M$.
Set $t = 1$, $U^{(global)}$=$max\{U^{(l)}(0, l = 1, \ldots, L)\}$
while $U^{(global)} < N$ **do**
  for $l = 1, \ldots, L$ **do**
    Compute $V^{(l)}(t), W^{(l)}(t), U^{(l)}(t)$
    if $U^{(l)}(t) > U^{(l,local)}(t)$ **then**
      $W^{(l,local)} = W^{(l)}(t), U^{(l,local)} = U^{(l)}(t)$
      if $U^{(l,local)} > U^{(global)}$ **then**
        $W^{(global)} = W^{(l,local)}$,
        $U^{(global)} = U^{(l,local)}$
    $t = t + 1$

TABLE I: Modeling parameters.

Parameter	Value
Deployment size (m^2)	100x100
Number of drone-cells	3
Number of UEs	100
UE height (m)	2
Drone-cell altitude (m)	30
UE speed (m/s)	1.4
Drone-cell speed (m/s)	8.3
TX power (dBm)	24
Power control scheme	Full-power
Number of BS array elements	8x8
Number of UE array elements	4x4
Frequency of beam-sweeping (μs)	3
Frame size (μs)	3
Type of transmission (UL and DL)	TDM
Carrier frequency (GHz)	73
Transmission bandwidth (GHz)	0.56
Packet size (byte)	3000
Traffic requirement (Mbps)	100
BS scheduler	Round-Robin

IV. Performance Evaluation

The numerical results and their analysis are described in this section. The following is divided into three parts. First, we discuss the network and geometry parameters of the considered scenario as well as briefly outline the utilized simulation tool. Next, we present the analytical results for a static drone-cell deployment and compare them with the simulation output as well as with the results of the adaptive navigation algorithm. Here, the emphasis is made on the comparison between the two discussed approaches. Finally, we report on the signal-to-interference-plus-noise ratio (SINR) values associated with the adaptive navigation algorithm.

A. Evaluation Methodology and System Parameters

The considered deployment area is assumed to be 100 by 100 meters. The drone-cell flight altitudes are fixed, while the drone-cells as well as the UEs are assumed to always reside in the deployment area. The choice of a fixed altitude of the drone-cells is justified by maximizing the coverage and signal strength for the UEs. Other parameters are summarized in Table I. The analytical results reported below are accompanied and complemented by those obtained with our system-level simulation (SLS) tool.

The SLS tool has the following capabilities. At the entity level, we construct the network, as well as create parameters, functions, and relationships between the modules. Further, supplementary system code generates traffic, handles the input and output operations, automates certain operations on the entity level, and provides libraries for other modules. The event subsystem handles the events according to their time and priority as well as synchronizes the physical layer (PHY) abstraction modules. PHY abstraction generates the channel model by taking into account a 3D antenna directivity pattern and calculates interference on the time-frequency transmis-

sions. In the end, data is stored in the database for further processing by the statistics rendering module. Most of the SLS code is written in Python.

To model a dynamic mmWave network, we created a dedicated module in the SLS, in which all of the discussed mmWave components are implemented. Here, for the sake of simulation simplicity, higher layers are abstracted with a simple packet-based traffic generator. We implemented a preliminary version of MAC, which emulates all the necessary procedures, including signal strength-based initial access and handover featuring 10 ms Time Division Multiplexing (TDM) frame (with 1 ms sub-frames) equally divided between the UL and the DL transmissions, as well as beam-sweeping and scheduling. The first two sub-frames of every frame are allocated for the control signaling, where the BS sends synchronization beacons, while the UEs may perform initial access and handover.

B. Coverage Analysis

Fig. 3a shows the proportion of covered UEs for the RDM model obtained by using SLS and analytical modeling for the random and fixed drone-cell deployments. It is easy to observe a close match between analysis and simulation for the grid deployment, in which the percentage of covered UEs fluctuates between 56% and 60%, whereas for a random drone-cell deployment it is only 24.4%. On average, the grid model performs better than a random drone-cell deployment. These results also confirm that for purely random mobility models there is no need for adaptive navigation of drone-cells.

Consider now the case of correlated mobility according to the RPGM model. Fig. 3b illustrates the proportion of covered UEs for RPGM in the grid deployment and adaptive navigation strategies. As one may observe, the percentage of covered UEs for the grid deployment decreases after 40 seconds of simulation time. Then, until the end of the simulation, it remains stable even though minor fluctuations caused by the mobility model still remain. On the other hand, adaptive navigation demonstrates 5% improvement on average. Furthermore, notice that the percentage of covered UEs changes periodically. It is explained by the navigation strategy that has been chosen: drone-cells take a "snapshot" of the current UE channel quality and then update their positions every 5 seconds according to the designed PSO algorithm.

C. SINR Analysis

While in this paper we primarily concentrate on the coverage analysis, the use of SLS allows to report on the SNR dynamics experienced by the UEs. Fig. 4a illustrates the SNR results obtained with SLS for the static grid deployment and adaptive navigation of drone-cells under the RDM model. Analyzing the data, we observe that adaptive navigation of drone-cells does not improve the SINR. Therefore, for this particular scenario, we can conclude that there is no need for a navigation strategy as predicted by the analytical results.

Fig. 4b reports simulation results for the static grid deployment and adaptive navigation of the drone-cells under the RPGM model. In contrast to Fig. 4a, we notice an improvement

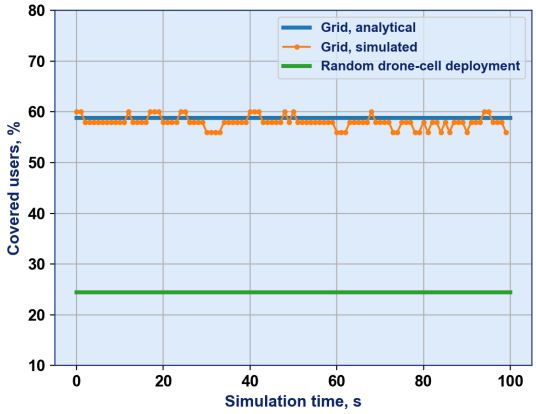

(a) Random Direction Mobility Model

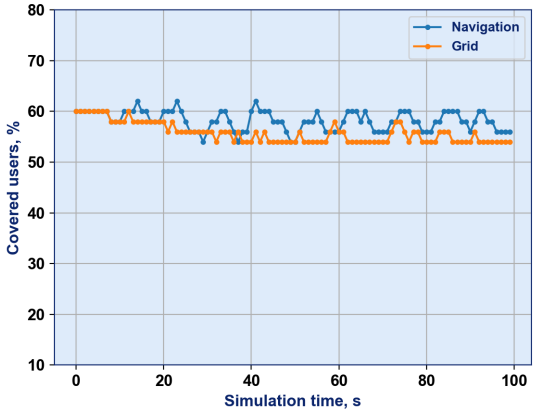

(b) Reference Point Group Mobility Model

Fig. 3: Proportion of covered UEs.

in the SINR for adaptive navigation as compared to the grid deployment. These differences are attributed to varying densities of UEs in the zone of interest for the two considered UE mobility models. In RDM, UEs are distributed uniformly across the deployment area and thus the average SINR and the coverage percentage do not change drastically over time. In RPGM, UEs are concentrated in enclosed spatial regions of the deployment area, thus decreasing the overall system performance on average.

V. Conclusion and Future Work

In this work, we investigated the impact of adaptive navigation of mmWave-based drone-cells for the RDM and RPGM user mobility models. The obtained results show that for the RDM model with a grid drone-cell deployment the number of covered UEs remains unchanged over time, thus implying that in purely random deployments there is no need for adaptive navigation. In correlated deployments, such as the one characterized by the group mobility, navigation leads to notable improvements in coverage and SNR performance as compared to a static grid deployment.

An adaptive navigation algorithm proposed in this paper employs information about the positions of all the UEs across

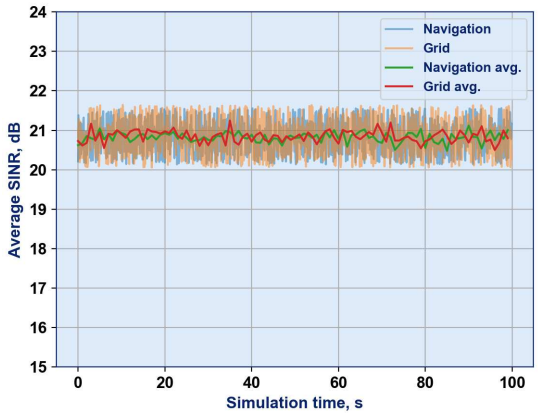

(a) Random Direction Mobility Model

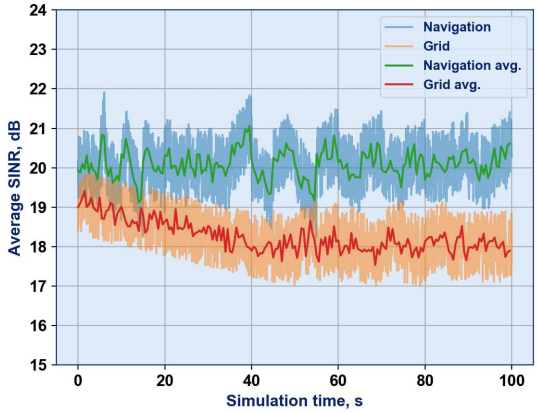

(b) Reference Point Group Mobility Model

Fig. 4: SINR variation over time.

the deployment area. This approach may be inefficient in larger scenarios with a high number of drone-cells. Our future work includes the development of a distributed algorithm to decrease the operational complexity in the system. We also plan to use more realistic trace-driven models of the UE mobility. For example, one scenario of interest may include a combination of pedestrian and vehicular traffic, by assuming realistic simulations of mmWave NLoS blockage. Finally, we intend to test various network optimization functions, which target to not only evaluate the coverage but also network capacity and drone-cell power consumption.

VI. Acknowledgment

This work was supported by Intel Corporation and by the Academy of Finland (project PRISMA). The authors are grateful to Jing Zhu and Feng Xue (Intel Corporation, USA) for valuable discussions and insightful comments that allowed to improve this paper.

References

[1] I. Bor-Yaliniz and H. Yanikomeroglu, "The new frontier in RAN heterogeneity: Multi-tier drone-cells," *IEEE Communications Magazine*, vol. 54, no. 11, pp. 48–55, 2016.

[2] Z. Xiao, P. Xia, and X.-G. Xia, "Enabling UAV cellular with millimeter-wave communication: Potentials and approaches," *IEEE Communications Magazine*, vol. 54, no. 5, pp. 66–73, 2016.

[3] M. Mozaffari, W. Saad, M. Bennis, and M. Debbah, "Drone small cells in the clouds: Design, deployment and performance analysis," in *Global Communications Conference (GLOBECOM), 2015 IEEE*, pp. 1–6.

[4] A. Al-Hourani, S. Kandeepan, and S. Lardner, "Optimal LAP altitude for maximum coverage," *IEEE Wireless Communications Letters*, vol. 3, no. 6, pp. 569–572, 2014.

[5] I. Bor-Yaliniz, A. El-Keyi, and H. Yanikomeroglu, "Efficient 3-D placement of an aerial base station in next generation cellular networks," in *Communications (ICC), 2016 IEEE International Conference on*, pp. 1–5.

[6] J. Sae, S. F. Yunas, and J. Lempiainen, "Coverage aspects of temporary LAP network," in *Wireless On-demand Network Systems and Services (WONS), 2016 12th Annual Conference on*, pp. 1–4, IEEE, 2016.

[7] E. Kalantari, H. Yanikomeroglu, and A. Yongacoglu, "On the number and 3D placement of drone base stations in wireless cellular networks," in *Vehicular Technology Conference (VTC-Fall), 2016 IEEE 84th*, pp. 1–6.

[8] M. Mozaffari, W. Saad, M. Bennis, and M. Debbah, "Efficient deployment of multiple unmanned aerial vehicles for optimal wireless coverage," *IEEE Communications Letters*, vol. 20, no. 8, pp. 1647–1650, 2016.

[9] E. Kalantari, M. Z. Shakir, H. Yanikomeroglu, and A. Yongacoglu, "Backhaul-aware robust 3D drone placement in 5G+ wireless networks," *arXiv preprint arXiv:1702.08395*, 2017.

[10] A. Fotouhi, M. Ding, and M. Hassan, "Dynamic base station repositioning to improve spectral efficiency of drone small cells," *arXiv preprint arXiv:1704.01244*, 2017.

[11] A. Fotouhi, M. Ding, and M. Hassan, "Dynamic base station repositioning to improve performance of drone small cells," in *Globecom Workshops (GC Wkshps), 2016 IEEE*, pp. 1–6.

[12] P. Nain, D. Towsley, B. Liu, and Z. Liu, "Properties of random direction models," in *INFOCOM 2005. 24th Annual Joint Conference of the IEEE Computer and Communications Societies. Proceedings IEEE*, vol. 3.

[13] F. Bai and A. Helmy, "A survey of mobility models," *Wireless Adhoc Networks. University of Southern California, USA*, vol. 206, p. 147, 2004.

[14] A. B. Constantine *et al.*, "Antenna theory: analysis and design," *MICROSTRIP ANTENNAS, John wiley & sons*, 2005.

[15] A. Al-Hourani, S. Kandeepan, and A. Jamalipour, "Modeling air-to-ground path loss for low altitude platforms in urban environments," in *Global Communications Conference (GLOBECOM), 2014 IEEE*, pp. 2898–2904.

[16] T. A. Thomas *et al.*, "3D mmwave channel model proposal," in *Vehicular Technology Conference (VTC Fall), 2014 IEEE 80th*.

[17] S. Verblunsky, "On the least number of unit circles which can cover a square," *Journal of the London Mathematical Society*, vol. 1, no. 3, pp. 164–170, 1949.

[18] R. Kershner, "The number of circles covering a set," *American Journal of mathematics*, vol. 61, no. 3, pp. 665–671, 1939.

[19] L. Santalo, *Integral Geometry and Geometric Probability*. Addison-Wesley, 1976.

[20] D. Moltchanov, "Distance distributions in random networks," *Ad Hoc Networks*, vol. 10, no. 6, pp. 1146–1166, 2012.

[21] S. N. Chiu, D. Stoyan, W. S. Kendall, and J. Mecke, *Stochastic geometry and its applications*. John Wiley & Sons, 2013.